CO_2 Reduction

International Edition: DOI: 10.1002/anie.201603034
German Edition: DOI: 10.1002/ange.201603034

Molybdenum–Bismuth Bimetallic Chalcogenide Nanosheets for Highly Efficient Electrocatalytic Reduction of Carbon Dioxide to Methanol

*Xiaofu Sun, Qinggong Zhu, Xinchen Kang, Huizhen Liu, Qingli Qian, Zhaofu Zhang, and Buxing Han**

Abstract: *Methanol is a very useful platform molecule and liquid fuel. Electrocatalytic reduction of CO_2 to methanol is a promising route, which currently suffers from low efficiency and poor selectivity. Herein we report the first work to use a Mo-Bi bimetallic chalcogenide (BMC) as an electrocatalyst for CO_2 reduction. By using the Mo-Bi BMC on carbon paper as the electrode and 1-butyl-3-methylimidazolium tetrafluoroborate in MeCN as the electrolyte, the Faradaic efficiency of methanol could reach 71.2 % with a current density of 12.1 mA cm^{-2}, which is much higher than the best result reported to date. The superior performance of the electrode resulted from the excellent synergistic effect of Mo and Bi for producing methanol. The reaction mechanism was proposed and the reason for the synergistic effect of Mo and Bi was discussed on the basis of some control experiments. This work opens a way to produce methanol efficiently by electrochemical reduction of CO_2.*

CO_2 is a cheap, abundant, and safe carbon resource, and its transformation into valuable chemicals and fuel has received much attention.[1,2] CO_2 conversion can be achieved by chemical methods, electrochemical reduction, and photocatalytic reduction.[3,4] The electrochemical reaction system is compact, modular, and the efficiency can be easily controlled by different parameters, such as electrode materials, electrolytes, and applied potentials.[5] The electrochemical reduction of CO_2 can proceed through two-, four-, six-, and eight-electron reduction pathways in different electrolytes over metals, metal complexes, and non-metallic electrodes, and the major products are CO,[6–9] formic acid/formate,[10–12] oxalic acid/oxalate,[13] methanol,[14] CH_4,[14–16] C_2H_4,[17] acetic acid/acetate,[18] as well as others.

Methanol is very important platform molecule for producing different chemicals and can also be used as fuel.[5,19,20] Some electrocatalysts, such as RuO_2-TiO_2, Ru/Cu, Cu and Mo, have proven to be effective for methanol production in CO_2 electrochemical reduction under mild conditions.[5,14,21–25] Pyridinium and its substituted derivatives are also active and stable homogeneous electrocatalysts to obtain methanol.[26–28] However, because electrochemical reduction of CO_2 to methanol deals with slow kinetics of multiple electron transfer, it is very difficult to achieve a high Faradaic efficiency of methanol formation, and the Faradaic efficiencies of all the routes reported up to date can only reach 40 % with reasonable current density (Supporting Information, Table S1). The unsatisfactory selectivity and high cost of electrodes are the main hindrance towards the industrial breakthrough of the processes. New heterogeneous catalysts are needed to advance this field.

Transition-metal dichalcogenides (TMDCs) have attracted significant interest owing to their fascinating mechanical, electrical, and optical properties.[29,30] As a representative material, MoS_2 has been widely used as efficient catalysts for hydrogen evolution, oxygen reduction, and hydrodesulfurization.[31,32] At present, there is a consensus that the MoS_2 catalytic activity originates mainly from the unsaturated S atoms along its edges. Increasing the number of exposed active sites on the edges and improving the electrical conduction are effective ways to enhance the electrocatalytic efficiency of MoS_2.[32] Introduction of doped atoms into MoS_2 may achieve this goal.

Herein we prepared different bimetallic chalcogenides (BMCs) and the BMCs on carbon paper (CP) were used as the electrodes for CO_2 electrochemical reduction to methanol. It was discovered that the Mo-Bi BMC/CP electrode was the most efficient when ionic liquid (IL), 1-butyl-3-methylimidazolium tetrafluoroborate ([Bmim]BF_4) in MeCN was used as the electrolyte, and methanol was the only liquid product. The Faradaic efficiency of methanol production could reach 71.2 % with a current density of 12.1 mA cm^{-2}, which is much higher than those reported in the literature. In addition, the reaction pathway was studied on the basis of control experiments.

The electrode materials were prepared via one-pot solvothermal reaction using ammonium tetrathiomolybdate and the other salt as precursors. To prepare the electrode, the BMCs with carbon black were suspended in ethanol with Nafion D-521 dispersion (5 wt %) to form a homogeneous ink assisted by ultrasound, which was spread onto carbon paper (CP) to get the BMC/CP electrodes.

Figure 1 shows the characterization results of the Mo-Bi BMC with Mo:Bi molar ratio of 1:1. Figure 1 A gives the scanning electron microscopy (SEM) image of the Mo-Bi BMC. The material has the sheet structure with an average lateral size of about 300 nm as determined by dynamic light scattering (DLS) method (Figure 1 B). The corresponding high-resolution transmission electron microscopy (HR-TEM) image (Figure 1 C) confirmed that both MoS_2 and Bi_2S_3

[*] X. Sun, Dr. Q. Zhu, X. Kang, Prof. Dr. H. Liu, Dr. Q. Qian, Dr. Z. Zhang, Prof. Dr. B. Han
Beijing National Laboratory for Molecular Sciences, Key Laboratory of Colloid and Interface and Thermodynamics, Institute of Chemistry Chinese Academy of Sciences, University of Chinese Academy of Sciences
Beijing 100190 (China)
E-mail: hanbx@iccas.ac.cn

Supporting information for this article can be found under: http://dx.doi.org/10.1002/anie.201603034.

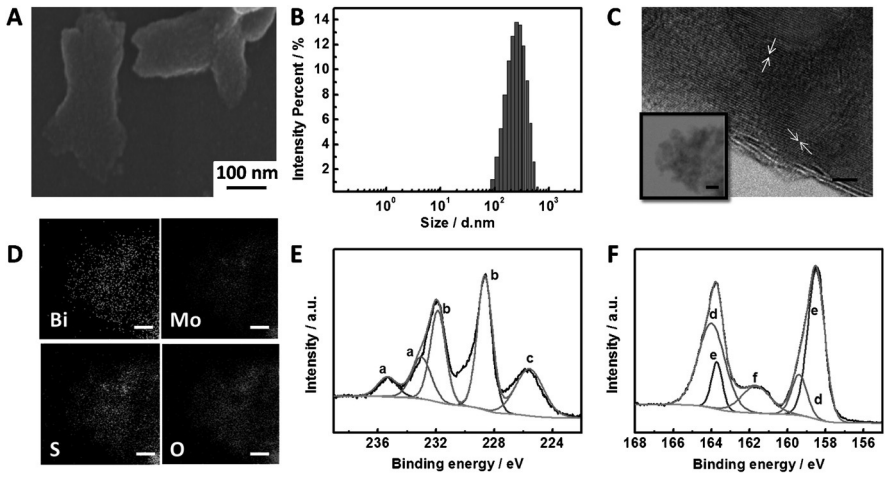

Figure 1. Structural and elemental analysis of the Mo-Bi BMC nanosheets with Mo:Bi molar ratio of 1:1. A) SEM image of the Mo-Bi BMC nanosheets. B) Size distribution (d = diameter) of the Mo-Bi BMC nanosheets in MeCN determined by dynamic light scattering (DLS). C) HR-TEM image of the nanosheets (scale bar: 2 nm). The white arrows show the crystal lattices of MoS_2 and Bi_2S_3. Inset of (C) and D) corresponding elemental mappings of the Mo-Bi BMC nanosheets (Inset of C: merged). The scale bar is 100 nm. E) and F) XPS spectra of Mo $3d_{3/2}$ (a), Mo $3d_{5/2}$ (b), S 2s (c), Bi $4f_{5/2}$ (d), Bi $4f_{7/2}$ (e), and S 2p (f) orbits of the Mo-Bi BMC nanosheets.

crystal lattices existed in the nanosheets, where 0.34 nm and 0.27 nm belong to the (130) plane of Bi_2S_3 and the (101) plane of MoS_2, respectively.[33,34] Elemental distribution mappings further illustrate the co-existence of Mo and Bi elements (Figure 1 D). X-ray photoelectron spectroscopy (XPS) spectra (Figures 1 E and F) show the chemical nature of the Mo-Bi BMC nanosheets, including the peaks belonging to Mo^{4+} (Mo $3d_{3/2}$: 235.3 and 232.9 eV; Mo $3d_{5/2}$: 231.8 and 228.6 eV), Bi^{3+} (Bi $4f_{5/2}$: 164.2 and 159.4 eV; Bi $4f_{7/2}$: 163.7 and 158.3 eV), and S (S 2s: 225.6 eV; S 2p: 161.6 eV).[33,35] The results provide direct evidence that the nanosheets are composed of MoS_2 and Bi_2S_3. The Mo 3d peaks also exhibit shifts compared to the pure MoS_2 nanosheet, providing further evidence for the strong interaction between MoS_2 and Bi_2S_3.

The present synthetic route could be extended to the preparation of other BMC nanosheets. By changing the guest metals Ag or Cu or without guest metal, Mo-Ag BMC or Mo-Cu BMC or MoS_2 nanosheets were prepared and the detailed characterizations are given in the Supporting Information, Figures S1–S3. The Mo-Ag BMC and Mo-Cu BMC nanosheets had similar structures to that of the Mo-Bi BMC.

The CO_2 reduction ability of the Mo-Bi BMCs was first examined by performing cyclic voltammetry (CV) measurements. The applied potential was swept between +0.8 and −1.4 V vs. standard hydrogen electrode (SHE) with a scan rate of 20 mV s^{-1}. The experiments were conducted in a typical three-electrode electrochemical H-cell using N_2 or CO_2-saturated MeCN containing 0.5 M $[Bmim]BF_4$ as an electrolyte at ambient temperature, which is a commonly used electrolyte.[7] As shown in Supporting Information, Figure S4, clear reduction peaks are observed for Mo-Bi BMC/CP (Mo:Bi molar ratio 1:1), Mo-Ag BMC/CP (Mo: Ag molar ratio 1:1), and Mo-Cu BMC/CP (Mo:Cu molar ratio 1:1) electrodes under CO_2 atmosphere, whereas no reduction peak appears in the absence of CO_2, indicating electrochemical reduction of CO_2 on the BMC/CP electrodes. The much higher current density of the CO_2-saturated system than the N_2-saturated indicates the reduction of CO_2.

Controlled potential electrolysis of CO_2 was performed at different applied potentials between −0.5 V and −1.1 V (vs. SHE) in CO_2-saturated MeCN containing 0.5 M $[Bmim]BF_4$ using a typical H-type cell (Supporting Information, Figure S5), which was similar to that used by other researchers.[12,15] Under the reported reaction conditions, methanol was the only liquid product as detected by nuclear magnetic resonance (NMR) spectroscopy, and CO, CH_4, and H_2 were the gaseous products determined by gas chromatography (GC). We also carried out experiment using labeled $^{13}CO_2$. The NMR spectra of the product (Figure S6) indicated that only $^{13}CH_3OH$ was produced, confirming that methanol was derived from CO_2. Figures 2 A–C show the current density and Faradaic efficiency for methanol, CO, CH_4, and H_2

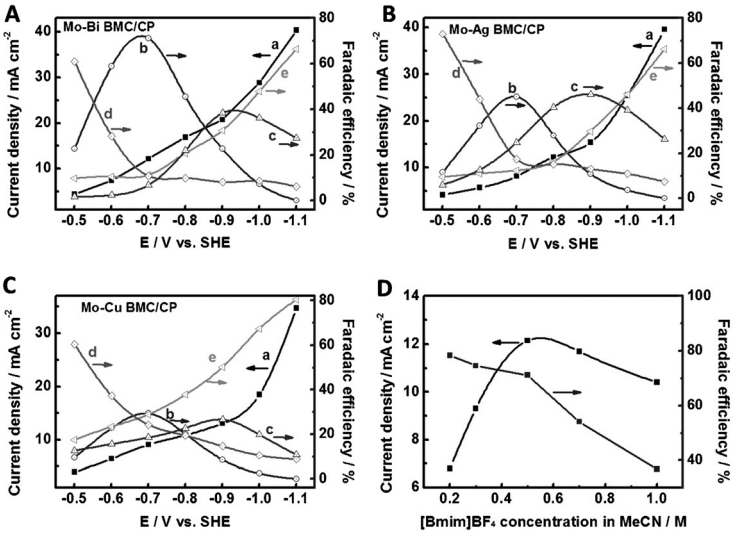

Figure 2. The current density and Faradaic efficiency of the products at different applied potentials over A) Mo-Bi BMC/CP electrode with Mo:Bi molar ratio 1:1, B) Mo-Ag BMC/CP electrode with Mo:Ag molar ratio of 1:1, and C) Mo-Cu BMC/CP electrode with Mo:Cu molar ratio of 1:1 in 0.5 M $[Bmim]BF_4$ MeCN solution saturated with 1 atm CO_2 at ambient temperature with 5 h electrolysis. Curve (a) is the current density; curves (b)–(e) are Faradaic efficiency of b) methanol, c) CH_4, d) CO, e) H_2, production. D) The Faradaic efficiency of methanol production and current density at −0.7 V (vs. SHE) as a function of $[Bmim]BF_4$ molar concentration in MeCN (M: mole L^{-}) over Mo-Bi BMC/CP electrode (Mo:Bi molar ratio of 1:1) with electrolysis time of 5 h.

production over the Mo-Bi BMC/CP, Mo-Ag BMC/CP, and Mo-Cu BMC/CP electrodes at different applied potentials.

It can be seen from Figure 2 that for all the three electrodes, the competitive hydrogen-evolution reaction (HER) is weak at low potentials and CO_2 reduction is prone to occur with the increasing applied potential. The maximum Faradaic efficiency of methanol occurred at −0.7 V (vs. SHE), but the performance of the Mo-Bi BMC/CP was clearly better than that of the Mo-Ag BMC/CP and Mo-Cu BMC/CP electrodes. The Faradaic efficiency of methanol production could reach 71.2% over Mo-Bi BMC/CP electrode with a current density of 12.1 mA cm^{-2}. The highest Faradaic efficiency of methanol reported in the literature was 55%, and the current density was only 0.05 mA cm^{-2}.[23] The reported Faradaic efficiency of methanol of the electrode/electrolyte systems with appreciable current density was much lower (Supporting Information, Table S1). We also used some other common supporting electrolytes in MeCN to perform the CO_2 electrochemical reduction, but their performances were not as good as [Bmim]BF_4 (Table S2).

The stability of the electrodes was tested with an electrolysis time of 5 h, and current density did not change obviously with time (Supporting Information, Figure S7). The long-term stability of the Mo-Bi BMC/CP electrode was also confirmed by XPS analysis before and after electrolysis (Supporting Information, Figure S8). The difference of the XPS spectra of the electrode before and after electrolysis process was not notable. All the results above indicate that Mo-Bi BMC/CP electrode and the IL-based electrolyte are excellent combination for electrochemical reduction of CO_2 to methanol.

At −0.7 V (vs. SHE), Mo-Bi BMC/CP is an effective electrode for the reduction of CO_2 to both methanol and CH_4. The change in Faradaic efficiency of methanol and CH_4 production with the applied potential originates from the differences in the CO_2 reduction mechanisms for generating the two chemicals. In principle, methanol and CH_4 may share some common intermediates. To produce methanol, a catalyst needs to break just one C–O bond in CO_2, while to produce CH_4, both of C–O bonds must be broken.[14] As Mo-Bi BMC could catalyze the formation of methanol effectively at lower potentials, the second C–O bond cleavage step to form CH_4 could occur at higher potential (Supporting Information, Figure S9). Figure 2 also shows that H_2 becomes the main product at much higher (that is, more negative) applied potential. The main reason may be that the rate of mass transport of H^+ is much faster than that of CO_2 in the electrolyte at high potential.

We investigated the effect of [Bmim]BF_4 concentration in the electrolyte on the electrolysis using Mo-Bi BMC/CP electrode (Figure 2D). The Faradaic efficiency of methanol decreased continuously with the increase of [Bmim]BF_4 concentration. The current density increased dramatically with increasing [Bmim]BF_4 concentration at the beginning, but decreased after the concentration exceeded 0.5 M. It is known that the conductivity of the electrolyte influences the current density of electrolysis significantly. Therefore, the effect of the IL on the current density can be explained roughly according to the influence of the IL on the conductivity. IL affects the electrolysis in two opposite ways.[36] The number of ionic species in the electrolyte increases with increasing IL concentration, which enhances the conductivity of the electrolyte. On the other hand, the viscosity of the electrolyte also increases with the addition of IL, which reduces the conductivity. In addition, IL can play a catalytic role on the CO_2 reduction with the stabilization of radical species including the $CO_2^{\bullet-}$, which can be recognized as a homogeneous electrocatalyst,[5] and the catalytic effect also depends on the concentration. The competition of these factors results in the maximum current density at 0.5 M.

Additionally, we also prepared a series of Mo-Bi BMC electrodes with different Mo:Bi molar ratios for CO_2 electrochemical reduction in 0.5 M [Bmim]BF_4 MeCN solution at −0.7 V (vs. SHE). As can be seen from Supporting Information, Figure S10, the molar ratio affected the Faradaic efficiency significantly, and the highest methanol Faradaic efficiency of methanol was obtained as the molar ratio of Mo:Bi was 1:1. Methanol was not generated when bulk MoS_2/CP or Bi_2S_3/CP electrode was used. H_2 was the major product over bulk MoS_2/CP electrode. CO and CH_4 became dominant products at higher Bi content. Mo-Ag/CP and Mo-Cu BMC/CP catalysts also showed the highest Faradaic efficiency of methanol when the molar ratio of the two metals was 1:1 (Figures S11,S12).

We determined the electrokinetic data in order to study the mechanism of the CO_2 reduction. The Tafel plots in Figure 3A shows the variation of overpotential with partial current density for methanol production over Mo-Bi BMC/CP electrode. The plot is linear in the overpotential range from 0.16 to 0.26 V with a slope of 124.4 mV dec^{-1}. This slope is consistent with a rate-determining initial electron transfer to CO_2 to form a surface-adsorbed $CO_2^{\bullet-}$ intermediate, which is a commonly accepted mechanism over metal electrodes.[37] Figure 3B shows IR spectra of the electrolyte phase after different electrolysis times over the Mo-Bi BMC/CP electrode in 0.5 M [Bmim]BF_4 MeCN solution at −0.7 V (vs. SHE). The signal of the original CO_2-saturated electrolyte is used as the background. Thus, absorption from the groups in the electrolyte was eliminated.[18] As expected, there is no peak from the IR spectra before the electrolysis. Some characteristic absorption bands can be observed during the process of electrolysis. The bands related to C–H and C–O appear at 1140 cm^{-1} and 1085 cm^{-1}, respectively, and the

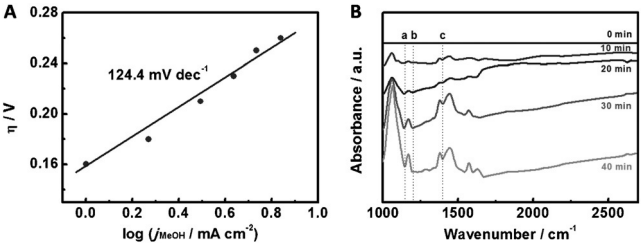

Figure 3. A) Tafel plot for methanol production over the Mo-Bi BMC/CP electrode with a Mo:Bi molar ratio of 1:1 in 0.5 M [Bmim]BF_4 MeCN electrolyte. B) IR spectra of the electrolyte phase in above electrode/electrolyte system at different electrolysis times and −0.7 V vs. SHE. (a: C–O, b: C–H, c: CH_3)

intensity increases with increasing electrolysis time. The appearance of the CH_3 peak at 1420 cm^{-2} indicates formation of methanol.

The high electrocatalytic selectivity of the Mo-Bi BMC/CP electrode can be attributed to the synergistic effect between Mo and Bi for producing methanol. Supporting Information, Figure S10B shows that the Bi-based electrode has high efficiency for conversion of CO_2 to CO, which is consistent with the conclusion reported by other authors.[7] In other words, Bi sites can efficiently drive CO generation in the presence of an IL. On the other hand, the Mo-based electrode is favorable for producing H_2, as can be seen from Supporting Information, Figure S10C. In addition, Mo sites can bind with CO,[23] which favors the further reduction of CO to methanol. Therefore, it can be deduced that Mo and Bi in the Mo-Bi BMC/CP electrode work synergistically for producing methanol because CO and H_2 can be produced on the electrode, the CO is bound and can be further hydrogenated to methanol. In addition, the better performance of Mo-Bi BMC than Mo-Ag and Mo-Cu BMC can be attributed to the ability of Bi sites for stabilizing $CO_2^{\bullet-}$ intermediates in the presence of IL.[7]

On the basis of the experimental results and the related knowledge in the literature, we propose a speculative mechanism for the electrochemical reduction of CO_2 to methanol over the Mo-Bi BMC/CP electrode, which is shown schematically in Supporting Information, Figure S13. In the first step, a complex $[Bmim\text{-}CO_2]^+$ can form quickly through the hydrogen bonding interaction between CO_2 and $[Bmim]^+$ cation.[38] This process may reduce the reaction barrier for electron transfer to CO_2, which plays a crucial role for reducing the overpotential of the reaction.[39] The complex can be adsorbed on the electrode surface and the CO_2 molecule is reduced to $CO_2^{\bullet-}$,[39,40] which can be inferred from the Tafel plot. The free-energy pathway becomes thermodynamically downhill to transfer the second electron to form adsorbed CO (CO_{ads}). Then, the CO_{ads} can be converted into CHO_{ads} after accepting an electron and proton. The protonation of CHO_{ads} leads to the formation of CH_3O_{ads} by capturing another two electrons. Finally, the downstream step is the transformation of CH_3O_{ads} to methanol after accepting the last electron and proton.

In summary, Mo-Bi BMC/CP with a Mo:Bi molar ratio of 1:1 is a very efficient and stable electrode for the electrochemical reduction of CO_2 to methanol. When 0.5 M $[Bmim]BF_4$ in MeCN is used as the electrolyte, the Faradaic efficiency for CO_2 electrochemical reduction to methanol can be as high as 71.2 % with a current density of 12.1 mA cm^{-2}, which is much higher than the values reported up to now. The high electrocatalytic selectivity of the Mo-Bi BMC/CP electrode can be attributed to the synergistic effect between Mo and Bi for producing methanol. The Bi enhances the transformation of CO_2 to CO, and the Mo favors the generation of H_2 and can bind CO. Thus, the CO is bound and can be further hydrogenated to obtain methanol. It may proceed with the pathway of $CO_2 \rightarrow CO_2^{\bullet-} \rightarrow CO_{ads} \rightarrow CHO_{ads} \rightarrow CH_3O_{ads} \rightarrow$methanol. This work provides a new and efficient route to produce methanol from CO_2.

Acknowledgements

We thank the National Natural Science Foundation of China (21133009, 21403253, 21533011, 21321063).

Keywords: bimetallic chalcogenides · carbon dioxide · electrocatalysis · nanosheets · ionic liquids

How to cite: *Angew. Chem. Int. Ed.* **2016**, *55*, 6771–6775
Angew. Chem. **2016**, *128*, 6883–6887

[1] M. He, Y. Sun, B. Han, *Angew. Chem. Int. Ed.* **2013**, *52*, 9620–9633; *Angew. Chem.* **2013**, *125*, 9798–9812.
[2] I. Dimitriou, P. Garcia-Gutierrez, R. H. Elder, R. M. Cuellar-Franca, A. Azapagic, R. W. K. Allen, *Energy Environ. Sci.* **2015**, *8*, 1775–1789.
[3] M. Aresta, A. Dibenedetto, A. Angelini, *Chem. Rev.* **2014**, *114*, 1709–1742.
[4] M. Alvarez-Guerra, J. Albo, E. Alvarez-Guerra, A. Irabien, *Energy Environ. Sci.* **2015**, *8*, 2574–2599.
[5] J. Qiao, Y. Liu, F. Hong, J. Zhang, *Chem. Soc. Rev.* **2014**, *43*, 631–675.
[6] B. Kumar, M. Asadi, D. Pisasale, S. Sinha-Ray, B. A. Rosen, R. Haasch, J. Abiade, A. L. Yarin, A. Salehi-Khojin, *Nat. Commun.* **2013**, *4*, 3819.
[7] J. L. DiMeglio, J. Rosenthal, *J. Am. Chem. Soc.* **2013**, *135*, 8798–8801.
[8] J. Shen, R. Kortlever, R. Kas, Y. Y. Birdja, O. Diaz-Morales, Y. Kwon, I. Ledezma-Yanez, K. J. P. Schouten, G. Mul, M. T. M. Koper, *Nat. Commun.* **2015**, *6*, 9177.
[9] D. Kim, J. Resasco, Y. Yu, A. M. Asiri, P. Yang, *Nat. Commun.* **2014**, *5*, 5948.
[10] S. Gao, Y. Lin, X. Jiao, Y. Sun, Q. Luo, W. Zhang, D. Li, J. Yang, Y. Xie, *Nature* **2016**, *529*, 68–71.
[11] N. Hollingsworth, S. F. R. Taylor, M. T. Galante, J. Jacquemin, C. Longo, K. B. Holt, N. H. de Leeuw, C. Hardacre, *Angew. Chem. Int. Ed.* **2015**, *54*, 14164–14168; *Angew. Chem.* **2015**, *127*, 14370–14374.
[12] S. Zhang, P. Kang, S. Ubnoske, M. K. Brennaman, N. Song, R. L. House, J. T. Glass, T. J. Meyer, *J. Am. Chem. Soc.* **2014**, *136*, 7845–7848.
[13] R. Angamuthu, P. Byers, M. Lutz, A. L. Spek, E. Bouwman, *Science* **2010**, *327*, 313–315.
[14] K. P. Kuhl, T. Hatsukade, E. R. Cave, D. N. Abram, J. Kibsgaard, T. F. Jaramillo, *J. Am. Chem. Soc.* **2014**, *136*, 14107–14113.
[15] X. Kang, Q. Zhu, X. Sun, J. Hu, J. Zhang, Z. Liu, B. Han, *Chem. Sci.* **2016**, *7*, 266–273.
[16] K. Manthiram, B. J. Beberwyck, A. P. Alivisatos, *J. Am. Chem. Soc.* **2014**, *136*, 13319–13325.
[17] F. S. Roberts, K. P. Kuhl, A. Nilsson, *Angew. Chem. Int. Ed.* **2015**, *54*, 5179–5182; *Angew. Chem.* **2015**, *127*, 5268–5271.
[18] Y. Liu, S. Chen, X. Quan, H. Yu, *J. Am. Chem. Soc.* **2015**, *137*, 11631–11636.
[19] J. Graciani, K. Mudiyanselage, F. Xu, A. E. Baber, J. Evans, S. D. Senanayake, D. J. Stacchiola, P. Liu, J. Hrbek, J. Fernandez Sanz, J. A. Rodriguez, *Science* **2014**, *345*, 546–550.
[20] F. Studt, I. Sharafutdinov, F. Abild-Pedersen, C. F. Elkjær, J. S. Hummelshøj, S. Dahl, I. Chorkendorff, J. K. Nørskov, *Nat. Chem.* **2014**, *6*, 320–324.
[21] J. Qu, X. Zhang, Y. Wang, C. Xie, *Electrochim. Acta* **2005**, *50*, 3576–3580.
[22] Y. Hori, A. Murata, R. Takahashi, S. Suzuki, *J. Chem. Soc. Chem. Commun.* **1988**, 17–19.
[23] D. P. Summers, S. Leach, K. W. Frese, Jr., *J. Electroanal. Chem.* **1986**, *205*, 219–232.

[24] M. Le, M. Ren, Z. Zhang, P. T. Sprunger, R. L. Kurtz, J. C. Flake, *J. Electrochem. Soc.* **2011**, *158*, E45 – E49.
[25] H. P. Yang, S. Qin, H. Wang, J. X. Lu, *Green Chem.* **2015**, *17*, 5144 – 5148.
[26] E. Barton Cole, P. S. Lakkaraju, D. M. Rampulla, A. J. Morris, E. Abelev, A. B. Bocarsly, *J. Am. Chem. Soc.* **2010**, *132*, 11539 – 11551.
[27] Y. Yan, E. L. Zeitler, J. Gu, Y. Hu, A. B. Bocarsly, *J. Am. Chem. Soc.* **2013**, *135*, 14020 – 14023.
[28] C. H. Lim, A. M. Holder, J. T. Hynes, C. B. Musgrave, *J. Am. Chem. Soc.* **2014**, *136*, 16081 – 16095.
[29] M. Asadi, B. Kumar, A. Behranginia, B. A. Rosen, A. Baskin, N. Repnin, D. Pisasale, P. Phillips, W. Zhu, R. Haasch, R. F. Klie, P. Král, J. Abiade, A. Salehi-Khojin, *Nat. Commun.* **2014**, *5*, 5470.
[30] X. Cui, G. H. Lee, Y. D. Kim, G. Arefe, P. Y. Huang, C. H. Lee, D. A. Chenet, X. Zhang, L. Wang, F. Ye, F. Pizzocchero, B. S. Jessen, K. Watanabe, T. Taniguchi, D. A. Muller, T. Low, P. Kim, J. Hone, *Nat. Nanotechnol.* **2015**, *10*, 534 – 540.
[31] S. Z. Butler, S. M. Hollen, L. Cao, Y. Cui, J. A. Gupta, H. R. Gutiérrez, T. F. Heinz, S. S. Hong, J. Huang, A. F. Ismach, E. Johnston-Halperin, M. Kuno, V. V. Plashnitsa, R. D. Robinson, R. S. Ruoff, S. Salahuddin, J. Shan, L. Shi, M. G. Spencer, M. Terrones, W. Windl, J. E. Goldberger, *ACS Nano* **2013**, *7*, 2898 – 2926.
[32] M. Xu, T. Liang, M. Shi, H. Chen, *Chem. Rev.* **2013**, *113*, 3766 – 3798.
[33] S. Wang, X. Li, Y. Chen, X. Cai, H. Yao, W. Gao, Y. Zheng, X. An, J. Shi, H. Chen, *Adv. Mater.* **2015**, *27*, 2775 – 2782.
[34] S. H. Song, B. H. Kim, D. H. Choe, J. Kim, D. C. Kim, D. J. Lee, J. M. Kim, K. J. Chang, S. Jeon, *Adv. Mater.* **2015**, *27*, 3152 – 3158.
[35] T. Liu, C. Wang, X. Gu, H. Gong, L. Cheng, X. Shi, L. Feng, B. Sun, Z. Liu, *Adv. Mater.* **2014**, *26*, 3433 – 3440.
[36] J. Zhang, W. Wu, T. Jiang, H. Gao, Z. Liu, J. He, B. Han, *J. Chem. Eng. Data* **2003**, *48*, 1315 – 1317.
[37] M. Gattrell, N. Gupta, A. Co, *J. Electroanal. Chem.* **2006**, *594*, 1 – 19.
[38] C. Cadena, J. L. Anthony, J. K. Shah, T. I. Morrow, J. F. Brennecke, E. J. Maginn, *J. Am. Chem. Soc.* **2004**, *126*, 5300 – 5308.
[39] B. A. Rosen, A. Salehi-Khojin, M. R. Thorson, W. Zhu, D. T. Whipple, P. J. A. Kenis, R. I. Masel, *Science* **2011**, *334*, 643 – 644.
[40] X. Sun, X. Kang, Q. Zhu, J. Ma, G. Yang, Z. Liu, B. Han, *Chem. Sci.* **2016**, *7*, 2883 – 2887.

Received: March 28, 2016
Published online: April 21, 2016

